ISBN: 978-3-95450-208-0 doi:10.18429/JACoW-IPAC2019-MOPTS019

END TO END SIMULATIONS AND ERROR STUDIES OF THE FAIR PROTON LINAC

Hendrik Hähnel*, Ulrich Ratzinger, Marc Syha and Rudolf Tiede
Institute for Applied Physics, Goethe University, Frankfurt, Germany
Carl M. Kleffner, GSI Helmholtzzentrum für Schwerionenforschung, Darmstadt, Germany

Abstract

The FAIR proton linac is developed as the high current proton injector for the future FAIR antiproton production chain at GSI [1]. It will provide a 70 mA proton beam at an energy of 68 MeV to the SIS18 synchrotron. The linac consists of an ECR ion source, followed by a ladder RFQ and a normalconducting linac based on CH-type cavities (see Fig. 1). High beam currents and strict beam quality requirements were the main drivers for the beam dynamics design. To ensure matching between the individual sections and validate the injector design as a whole, end to end simulations were performed using TraceWin [2, 3] with 3D fieldmaps of the CH-linac. In this paper, the final cavity design, as well as the results of end to end simulations and error studies are discussed.

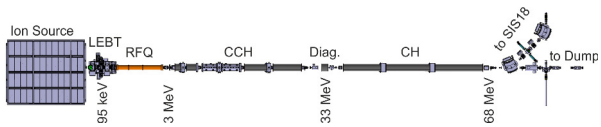

Figure 1: Layout of the FAIR proton linac.

Following the ECR ion source, a novel ladder-RFQ [4, 5] accelerates the protons up to 3 MeV. To reach the desired end-energy of 68 MeV, six CH – type cavities are used in combination with KONUS beam dynamics [6]. A diagnostics section with a 6-gap buncher is positioned in the middle of the linac at 33 MeV. In total, 12 quadrupole triplets are needed for transverse focusing along the CH-linac.

CH-TYPE CAVITY DESIGN

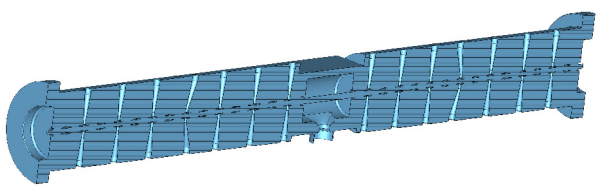

Figure 2: Vaccuum model of the third CCH-cavity.

The cavity design of all six CH-type cavities has been finalized at IAP Frankfurt recently. The first three cavities each include an internal quadrupole triplet lens. The lens sits in a coupling cell in the center of the cavities. Therefore, these cavities are called "Coupled CH-cavities", short CCH. While the coupling cells initially had a cylindrical shape

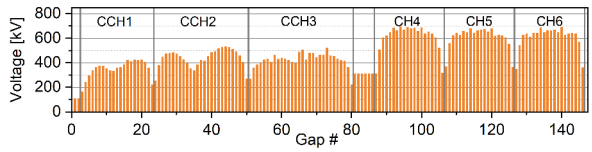

Figure 3: Effective voltage distribution of all six CH-type cavities and two buncher cavities.

[7, 8], this had to be changed for ease of installation of the internal triplet lenses. Now, the coupling cells have a flat top and bottom shape and the top can be opened to insert the lens (see Fig. 2). This has the positive side effect, that maintenance of the internal triplet lenses is made easier.

Table 1: Final Cavity Parameters of the CH-Linac

	CCH1	CCH2	CCH3
P_{loss} [MW]	0.73	1.02	1.02
P_{beam} [MW]	0.52	0.83	0.89
P_{tot} [MW]	1.25	1.85	1.91
Z_{eff} [MΩ/m]	52.3	54.5	43.7
L_{tank} [m]	1.45	2.56	3.65
	CH4	CH5	CH6
P_{loss} [MW]	1.35	1.31	1.25
P_{beam} [MW]	0.85	0.85	0.85
P_{tot} [MW]	2.2	2.16	2.11
Z_{eff} [MΩ/m]	42	38.6	36.9
L_{tank} [m]	2.62	2.95	3.23

However, the ramifications of these changes on the RF design were not trivial. While the radius of the coupling cell was increased to compensate for the lost volume due to the lid, the distance between the lens top and the outer tank wall was significantly reduced. Therefore, the coupling cell geometry had to be carefully tuned to keep the desired voltage distribution along with the mode separation to the neighboring mode. The final voltage distribution for all six CH-type cavities is shown in Fig. 3. In Addition, the final cavity parameters are summarized in Tab. 1.

END TO END SIMULATIONS

To verify the beam dynamics design of the FAIR proton linac, end to end simulations were performed using TraceWin. These simulations include the RFQ, as well as the CH-linac section. The input beam was chosen to be a 4D waterbag in front of the RFQ with a total of $2.5 \cdot 10^4$

* haehnel@iap.uni-frankfurt.de

ISBN: 978-3-95450-208-0 doi:10.18429/JACoW-IPAC2019-MOPTS019

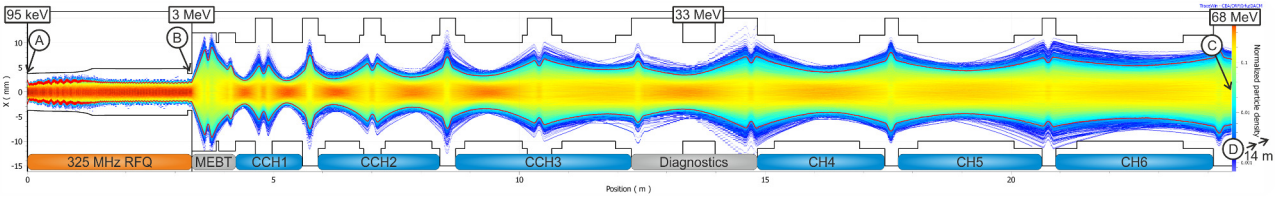

Figure 4: Horizontal beam density of the FAIR proton linac end to end simulations. The particle density colormap is scaled logarithmic. The dark blue edge of the beam amounts to about $2 \cdot 10^{-3}$ of all particles.

macroparticles and a beam current of 75 mA. The transverse normalized rms emittance of the input beam is 0.3 mm mrad and the energy spread $\Delta W/W = 10^{-3}$. The RFQ beam was then matched into the following linac by the MEBT section. The CH-linac was simulated with 3D fieldmaps of all cavities, obtained from the final CST simulations. The fieldmaps were generated with a step size of 0.5 mm and cover the full drift-tube aperture within the cavities. The two buncher cavities (MEBT and 33 MeV diagnostics section) are modeled using the thin-gap approximation in TraceWin. The end to end simulation ends behind the last external triplet lens of the linac. An additional simulation of a simplified transport and debuncher was done separately.

An evolution of the proton beam along the linac is shown in the cluster plots in Fig. 7 from (A) to (D).

RFQ

The simulation of the RFQ was performed using the Toutatis code within TraceWin, with imported RFQ vane geometry for the best agreement between the original RFQGen simulations [5] and the end to end simulations. The simulation results are in good agreement and have been verified for different particle numbers and beam currents [9]. Transmission of the RFQ in end to end simulations is 93.9 %.

CH-Linac

The new 3D fieldmap based simulations of the CH-linac section show better final rms emittances than the LORASR design simulations[1]. In the transverse plane, this is due to much lower emittance growth in the CH-linac section (see Fig. 5). In the longitudinal plane, the initial emittance of the LORASR design is larger than the emittance produced by the RFQ. Therefore, the RFQ stays within the acceptance of the

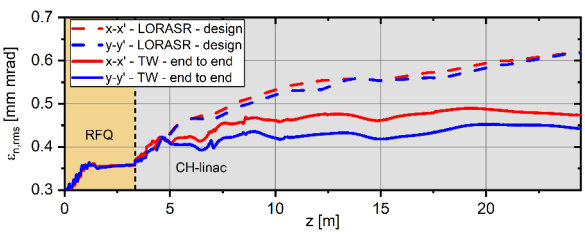

Figure 5: Transverse rms emittance of the end to end simulation, compared with the LORASR design simulation for the CH-linac section.

[1] The LORASR design simulations use a 6D waterbag distribution as input.

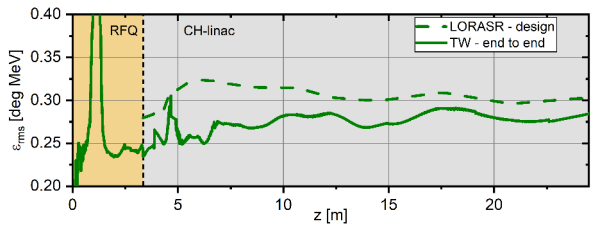

Figure 6: Longitudinal rms emittance of the end to end simulation, compared with the LORASR design simulation. In the RFQ section, the plot is cut at 0.4 deg MeV for visibility.

linac and longitudinal emittance growth is low (see Fig. 6), even though, the RFQ output distribution is not perfectly symmetrical (as shown in Fig. 7 (B)). The total transmission behind the CH-linac is 93.7 %, and therefore a final beam current of 70.2 mA is achieved.

Debuncher

The injection into the SIS18 synchrotron sets strict requirements on the linac beam emittances and energy spread [10, 11]. To asses the achievable energy spread of the FAIR proton linac, the beam from the end to end simulations was tracked an additional 14 meters after which it passed a 6-gap debuncher cavity. The resulting particle distribution behind the debuncher is shown in Fig. 7 (D). The achieved rms energy spread behind the debuncher is

$$\Delta W/W = \pm 2.2 \cdot 10^{-4} \ (\Delta p/p = \pm 1.14 \cdot 10^{-4}),$$

which is well within the desired range of $\Delta \leq 0.5 \cdot 10^{-3}$(rms) [12, 13].

ERROR STUDIES

Table 2: Parameters for the CH-Linac Error Study (2σ).

Lenses	**Singlets**	**Triplets**
Δxy	$\pm 100\,\mu$m	$\pm 150\,\mu$m
$\Delta\phi_{x,y,z}$	± 2 mrad	± 2 mrad

RFQ Beam		**Cavities**	
Δxy	$\pm 100\,\mu$m	Δxy	$\pm 150\,\mu$m
$\Delta W/W_0$	± 2 %	Δxy_{gap}	$\pm 150\,\mu$m
$\Delta\phi_{x,y,z}$	± 2 mrad	ΔV_{gap}	± 1 %
$\Delta\phi_0$	± 1 deg	$\Delta E/E_0$	± 1 %
		$\Delta\phi_s$	± 1 deg

ISBN: 978-3-95450-208-0 doi:10.18429/JACoW-IPAC2019-MOPTS019

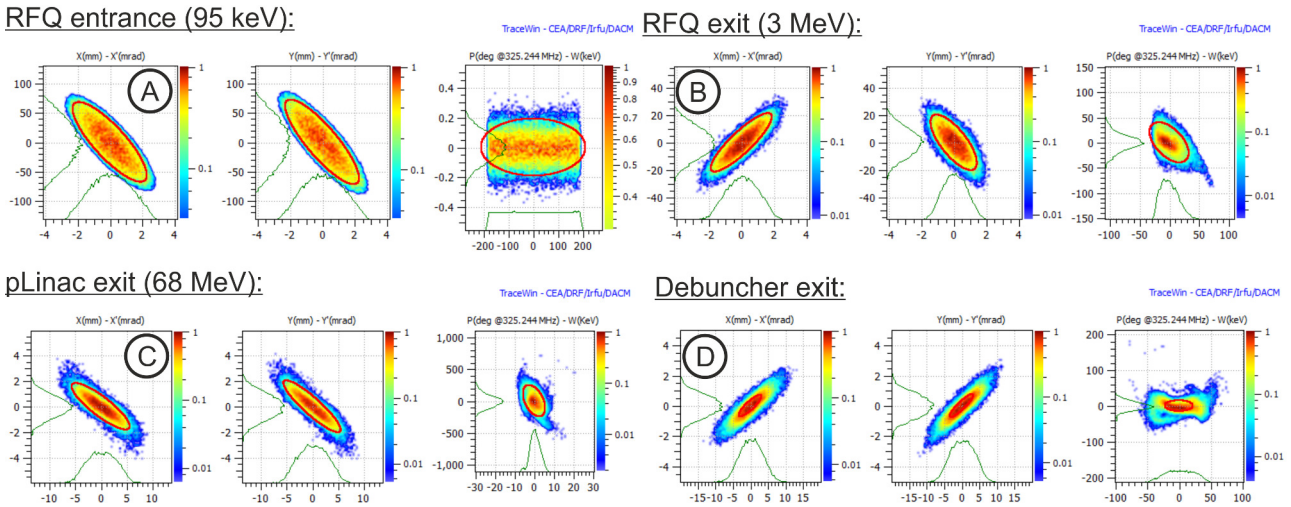

Figure 7: Evolution of the proton beam along the FAIR proton linac from position (A) to (D), as denoted in Fig. 4.

The stability of a linac design is a major concern for real world operation. Previous error studies of the CH-linac have been performed with LORASR [14]. More recently, detailed error studies have been carried out using a TraceWin model of the linac (thin gap). The resulting average transmission for a realistic set of errors is shown in Fig. 8 (parameters in Tab. 2). Future investigations will take advantage of the new fieldmap linac model portrayed above.

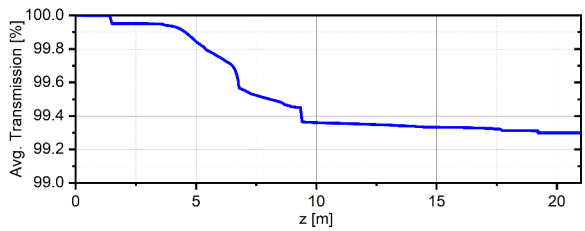

Figure 8: Average losses along the CH-linac from error studies.

Recent studies [15, 16] showed, that it is very important to treat quadrupole singlet and triplet errors independently. This has also been confirmed during error studies of the FAIR proton linac.

Acceptable error levels are in the order of:

Singlets: $\Delta xy = \pm 50\text{–}100\,\mu\text{m}$, $\Delta\phi_{x,y,z} = \pm$several mrad

Triplets: $\Delta xy = \pm 100\text{–}500\,\mu\text{m}$, $\Delta\phi_{x,y,z} = \pm$few mrad

CONCLUSION

New fieldmap based simulations of the CH-linac in combination with simulations of the RFQ show better than expected performance for the FAIR proton linac. Both longitudinal and transverse emittances at the linac exit are lower than the design values. At 75 mA, a total transmission of 93.6 % is achieved.

ACKNOWLEDGEMENTS

The author would like to acknowledge the open minded and fruitful cooperation with the pLinac team at GSI Darmstadt. Special thanks are also extended to Ali Almomani for his previous work on the project and the support given during the transition phase at IAP.

APPENDIX

Some Notes on Code Comparisons

During the comparison of TraceWin thin-gap, TraceWin fieldmap, and LORASR simulations of the FAIR proton linac, the following observations were made. Longitudinal emittance growth with the same 6D waterbag distribution is highest in TraceWin thin-gap simulations, while the TraceWin fieldmap simulations and LORASR are very similar. It is believed, that the movement of the bunch in longitudinal phase space is least accurately described by the thin-gap method. It seems, that the complexity of KONUS beam dynamics, in combination with short gap geometries, where the accelerating field may reach halfway into the drifttube, may be an edge-case, where the limits of this approximation can be observed. The stepwise tracking of the bunch motion within the accelerating gap in LORASR accounts for these cases and is therefore believed to be a more accurate representation of the longitudinal beam motion. Any attempts to reproduce the exact gap center phases and energies of a LORASR or fieldmap simulation using the one-step-per-gap method may therefore be flawed by design.

Transverse emittance growth however is similar for both types of TraceWin simulations and higher in LORASR simulations. Here, the radial accuracy of the parametric fieldmaps in LORASR might be not granular enougth and produce unneccessary emittance growth. Particle losses may also play a role here.

The author wants to stress, that these observations are in no way a final judgement and warrent further investigation.

ISBN: 978-3-95450-208-0 doi:10.18429/JACoW-IPAC2019-MOPTS019

REFERENCES

[1] C. M. Kleffner *et al.*, "Status of the FAIR Proton Linac", presented at the 10th Int. Particle Accelerator Conf. (IPAC'19), Melbourne, Australia, May 2019, paper MOPTS020, this conference.

[2] TraceWin, http://irfu.cea.fr/dacm/logiciels/

[3] D. Uriot and N. Pichoff, "Status of TraceWin Code", in *Proc. 6th Int. Particle Accelerator Conf. (IPAC'15)*, Richmond, VA, USA, May 2015, pp. 92–94. doi:10.18429/JACoW-IPAC2015-MOPWA008

[4] M. Schuett, U. Ratzinger, and M. Syha, "RF Measurements and Tuning of the 325 MHz Ladder-RFQ", presented at the 10th Int. Particle Accelerator Conf. (IPAC'19), Melbourne, Australia, May 2019, paper MOPTS033, this conference.

[5] M. Syha, H. Hähnel, U. Ratzinger, and M. Schuett, "New Beam Dynamics Simulations for the FAIR p-Linac RFQ", presented at the 10th Int. Particle Accelerator Conf. (IPAC'19), Melbourne, Australia, May 2019, paper MOPTS032, this conference.

[6] R. Tiede, H. Hähnel, and U. Ratzinger, "Beam Dynamics Design Parameters for KONUS Lattices", in *Proc. 8th Int. Particle Accelerator Conf. (IPAC'17)*, Copenhagen, Denmark, May 2017, pp. 683–685. doi:10.18429/JACoW-IPAC2017-MOPIK068

[7] C. M. Kleffner *et al.*, "Status of the FAIR pLinac", in *Proc. 8th Int. Particle Accelerator Conf. (IPAC'17)*, Copenhagen, Denmark, May 2017, pp. 2208–2210. doi:10.18429/JACoW-IPAC2017-TUPVA058

[8] Ali M. Almomani et al., "Updated cavities design for the FAIR p-linac", J. Phys.: Conf. Ser., 874 012046, 2017.

[9] M. Syha, private communication, April 2019.

[10] S. Appel, O. Boine-Frankenheim and F. Petrov, "Injection optimization in a heavy-ion synchrotron using genetic algorithms", Nucl. Instr. and Meth. A 852 73–79, 2017. DOI: http://dx.doi.org/10.1016/j.nima.2016.11.069

[11] S. Appel, et al., "Optimization of Heavy-Ion Synchrotrons Using Nature-Inspired Algorithms and Machine Learning", presented at the 13th International Computational Accelerator Physics Conference (ICAP'18), Key West, Florida, USA, Oct. 2018, paper SAPAF02.

[12] S. Appel, "Longitudinal beam quality",presented at pLinac project meeting, GSI Darmstadt, April 2019, unpublished.

[13] S. Appel, O. Boine-Frankenheim, "Microbunch dynamics and multistream instability in a heavy-ion synchrotron", Phys. Rev. ST Accel. Beams 15, 054201, 2012.

[14] R. Tiede, A. Almomani, M. Busch, F. D. Dziuba, and U. Ratzinger, "Improved Beam Dynamics and Cavity RF Design for the FAIR Proton Injector", in *Proc. 28th Linear Accelerator Conf. (LINAC'16)*, East Lansing, MI, USA, Sep. 2016, pp. 111–113. doi:10.18429/JACoW-LINAC2016-MOPRC018

[15] H. Hähnel, "Development of an IH-Type Linac for the Acceleration of High Current Heavy Ion Beams", PhD thesis, Goethe University, Frankfurt, Germany, 2017. http://d-nb.info/1137944528/34

[16] H. Hähnel, U. Ratzinger, R. Tiede, "The KONUS IH-DTL proposal for the GSI UNILAC poststripper linac replacement", J. Phys.: Conf. Ser., 874 012047, 2017. doi:10.1088/1742-6596/874/1/012047